Supplementary Information for:

Solution Aggregation of Platinum(II) Triimine Methyl Complexes

Vikas M. Shingade*, William B. Connick#

Department of Chemistry, University of Cincinnati, P.O. Box 210172, Cincinnati, Ohio 45221-0172

*E-mail: vikas.shingade@gmail.com
deceased

Table of Contents **Pages**

EXPERIMENTAL

A) Materials and methods

Potassium tetrachloroplatinate(II), K_2PtCl_4, was purchased from Pressure Chemical Co. (Pittsburgh, PA). 2,2′:6′,2″-terpyridine, dimethyl sulfide, and 1.4 m solution of methyllithium (halide content ca. 0.05 M) in diethyl ether, ammonium hexafluorophosphate were obtained from Sigma-Aldrich, whereas N-Methyl-1,2-phenylenediamine and 2,6-Pyridinedicarboxylic acid and Spectroscopic grade dimethyl sulfoxide were obtained from Acros Organics and used as received unless specified otherwise. Deuterated solvents were purchased from Cambridge Isotope Laboratories. The ligand, 2,6-Bis(N-methylbenzimidazol-2-yl)pyridine (mbzimpy)[1], and the platinum synthon, Chloromethyl-bis-(dimethyl sulfide) Platinum (II), [Pt(SMe_2)(Me)Cl], were prepared in highly pure form according to published procedures[2-5] and under an inert atmosphere of argon using standard Schlenk techniques. Argon was pre-dried using activated sieves, and trace impurities of oxygen were removed with activated R3-11 catalyst from Schweizerhall. [Pt(tpy)CH_3](PF_6) (**1**) and [Pt(mbzimpy)CH_3](PF_6) (**2**) were prepared in analytically pure form following the modifications of the published procedure for **1**.[4] Elemental analyses were performed by Atlantic Microlab (Norcross, GA). The 1D (^{1}H, ^{13}C, and ^{195}Pt) and 2D (COSY, HSQC, and NOESY) NMR spectra were recorded at room-temperature (20-25 °C). In the case of **1**, a series of ^{195}Pt NMR spectra were recorded over the temperature range of 25-70 °C. 2D NOESY experiments were run with mixing time, τ_m, of 75 ms at room-temperature. Spectra are reported in parts per millions (ppm) relative to TMS (δ = 0 ppm), or the residual internal standard (~ the protic solvent impurity) [$(CD_3)_2SO$, δ_H = 2.50 ppm; and δ_C = 39.52 ppm for

$CD_3SOCD_2H)]$[6], or relative to a saturated solution of $Na_2[PtCl_6]$ in D_2O in the case of ^{195}Pt NMR.

B) Instrumentation

The ^1H, ^{13}C, COSY, and HSQC NMR spectra were recorded using Bruker AC 400 MHz instrument, whereas NOE and ^{195}Pt NMR spectra were recorded using a Bruker DMX 500 MHz and a Bruker AMX 400 MHz instruments, respectively. Mass spectra were obtained by electrospray ionization using either an Ionspec HiRes ESI-FTICRMS instrument or a Micromass Q-TOF-II instrument. The instrument conditions were optimized and calibrated in positive ion mode using poly-alanine (Sigma) and in negative ion mode using sodium iodide (Fisher Scientific). The observed isotope patterns agreed well with those predicted based on natural isotopic abundances (only monoisotopic masses are provided here). UV-visible absorption spectra were recorded using an HP8453 diode array spectrometer on samples contained in 1 cm and 1 mm pathlength quartz cuvettes.

C) Syntheses and Characterization

[*Note*: We recently have published 'syntheses and characterization' of mbzimpy, and compounds **1** and **2** in Dalton Transactions (Shingade *et al.*, *Dalton Trans.*, 2020, DOI: 10.1039/d0dt01496f). A portion of this section we have replicated here to provide easy access to that information][7]

2,6-bis(N-methylbenzimidazol-2'-yl)pyridine **(mbzimpy).** Synthesis of mbzimpy was adapted from Addison *et al.,*[1] and optimized for reaction conditions. N-methyl-1,2-phenylenediamine (0.73 g, 6.0 mmol) was added to 10 ml of aqueous orthophosphoric acid (85 %) under vigorous magnetic stirring, followed by addition of 2,6-pyridinedicarboxylic acid (0.50 g, 3.0 mmol). The reaction mixture was refluxed under argon at 250 °C (using a sand bath) for 24 h. The resulting solution, upon cooling down to room temperature, was added drop-wise to an ice-cold aqueous

solution of potassium hydroxide (~1 M, 100 mL). The flask was then chilled in an ice-water-bath for at least 2 h. The mbzimpy precipitate filtered off and washed with ice-cold distilled water. The product was further purified by recrystallization from acetone: water (~ 90:10) solution. Glassy-white needles with a light bluish hue were obtained by slow evaporation of the solvent mixture. Yield: 0.91 g, 90 %. MS-ESI (m/z): 340.15 ($C_{21}H_{17}N_5H^+$), Calcd., 340.16. ^{1}H NMR (400 MHz, 3.0 mM, $(CD_3)_2SO$, 298 K, δ/ppm) δ_H 8.41 (2H, d, ^3J = 7.6 Hz, H_3), 8.23 (1H, t, ^3J = 7.4 Hz, H_4), 7.78 (2H, d, ^3J = 8.0 Hz, $H_{4'}$ and $H_{4''}$), 7.71 (2H, d, ^3J = 8.0 Hz, $H_{7'}$ and $H_{7''}$), 7.38 (2H, dd, ^3J = 7.2 Hz, $H_{6'}$ and $H_{6''}$), 7.32 (2H, dd, ^3J = 7.2 Hz, $H_{5'}$ and $H_{5''}$), 4.27 (6H, s, N-CH_3). ^{13}C NMR (400 MHz, 54 mM in $(CD_3)_2SO$, 298 K, δ/ppm) δc 149.7, 149.2, 141.9, 138.6(C_4), 137.1, 125.1 (C_3), 123.4 ($C_{6'}$ and $C_{6''}$), 122.6 ($C_{5'}$ and $C_{5''}$), 119.5 ($C_{4'}$ and $C_{4''}$), 111.0 ($C_{7'}$ and $C_{7''}$), 32.6 (N-CH_3).

[Pt(mbzimpy)CH_3](PF_6) (2). Synthesis of $PtClMe(SMe_2)_2$ was adapted from Hill *et al*.[4] A mixture of mbzimpy (0.16 g, 0.47 mmol) and $PtClMe(SMe_2)_2$ (0.2 g, 0.47 mmol) in 50 mL methanol was sonicated for 6 h at room temperature to give a red solution. The resultant solution was filtered, and the filtrate was reduced in volume to 2 mL under vacuum. Upon addition of 25 mL diethyl ether, the mixture was then chilled in a dry-ice/acetone bath for 1 hour. The resultant red precipitate was isolated by filtration, and then washed successively with dichloromethane and diethyl ether. An orange-red $(PF_6)^-$ salt of **2** was prepared by metathesis using a saturated aqueous solution of NH_4PF_6. Yield: 0.22 g, 80 %. MS-ESI (m/z): 549.14 $(PtC_{22}H_{20}N_5)^+$. Anal. Calcd. for $C_{22}H_{20}F_6N_5PPt$: C, 38.05; H, 2.9; N, 10.08. Found: C, 38.28; H, 2.9; N, 10.22. ^{1}H NMR (400 MHz, 0.67 mM in $(CD_3)_2SO$, 298 K, δ/ppm) δ_H 8.59 (2H, d, ^3J = 7.8 Hz, H_3), 8.52 (1H, t, ^3J = 7.8 Hz, H_4), 7.93 (4H, d, ^3J = 8.2 Hz, $H_{4'}$, $H_{4''}$, $H_{7'}$ and $H_{7''}$), 7.59 (4H, m, $H_{5'}$, $H_{5''}$, $H_{6'}$

and $H_{6''}$), 4.36 (6H, s, N-CH_3), 1.98 (3H, s, $^2J_{Pt\text{-}H}$ = 79.2 Hz, Pt-CH_3). ^{13}C NMR (400 MHz, 29.4 mM in $(CD_3)_2SO$, 298 K, δ/ppm) δ_c 154.1, 144.6, 140.8 (C_4), 138.7, 134.0, 126.1; 125.3 ($C_{5'}$; $C_{5''}$, and $C_{6'}$; $C_{6''}$), 124.1 (C_3), 115.4; 112.1 ($C_{4'}$; $C_{4''}$, and $C_{7'}$; $C_{7''}$), 32.3 (N-CH_3), -25.6 (Pt-CH_3). ^{195}Pt NMR (400 MHz, 48 mM, $(CD_3)_2SO$, 298 K, δ/ppm) δ -3346.2

[Pt(tpy)CH_3](PF_6) (1).[8, 9] An orange-red product was isolated following the synthetic procedure for **2** from $PtClMe(SMe_2)_2$ and substituting tpy for mbzimpy. Orange-red crystals were obtained upon slow evaporation from acetone: water (90:10) solution. Yield: 0.26, 84%. Anal. Calcd. for $C_{16}H_{14}F_6N_3PPt$: C, 32.66; H, 2.40; N, 7.14. Found: C, 32.88; H, 2.28; N, 7.33.^{1}H NMR (400 MHz, 1.5 mM in $(CD_3)_2SO$, 298 K, δ/ppm) δ 8.91 (2H, d, ^3J = 5.6 Hz, $J_{Pt\text{-}H}$ = 49.6 Hz, H_6 and $H_{6''}$), 8.62-8.67 (4H, d, ^3J = 8.4 Hz), 8.55 (1H, t, ^3J = 8.4 Hz), 8.47 (2H, dd, ^3J = 7.8 Hz), 7.87 (2H, dd, ^3J = 6.4 Hz), 1.10 (3H, s, $^2J_{Pt\text{-}H}$ = 73.2 Hz, Pt-CH_3). ^{1}H NMR (400 MHz, 240 mM in $(CD_3)_2SO$, 298 K, δ/ppm) δ 7.96 (2H, dd), 7.85-7.65 (7H, m), 7.30 (2H, dd), -0.08 (3H, s). ^{13}C NMR (400 MHz, 240 mM in $(CD_3)_2SO$, 298 K, δ/ppm) δ 157.9, 150.5, 150.1, 140.7, 139.8, 128.5, 125.0, 123.05, -5.14. ^{195}Pt NMR (400 MHz, 79.8 mM in $(CD_3)_2SO$, 298 K, δ/ppm) δ -3198.4 (~25 °C); -3194.0 (50 °C); -3189.0 (70 °C).

Table S1: Electronic absorption data for **1** and **2** in dimethyl sulfoxide at room-temperature.[7]

Compounds	**Absorbance λmax nm (ε, M^{-1} cm^{-1})**
[Pt(mbzimpy)CH_3](PF_6)	314 (26 261), 346 (25 401), 367sh (19 485), 468sh (561) 468 [cd], ~560 [cd]
[Pt(tpy)CH_3](PF_6)	316 (12 797), 326 (12 197), 340 (13 710), 356sh (5 785), 386sh (1 892), 408 (2 482), 425sh (1 920), 477[cd], 520 [cd], ~ 560[cd]

[cd]: concentration dependent absorptions, sh: shoulder

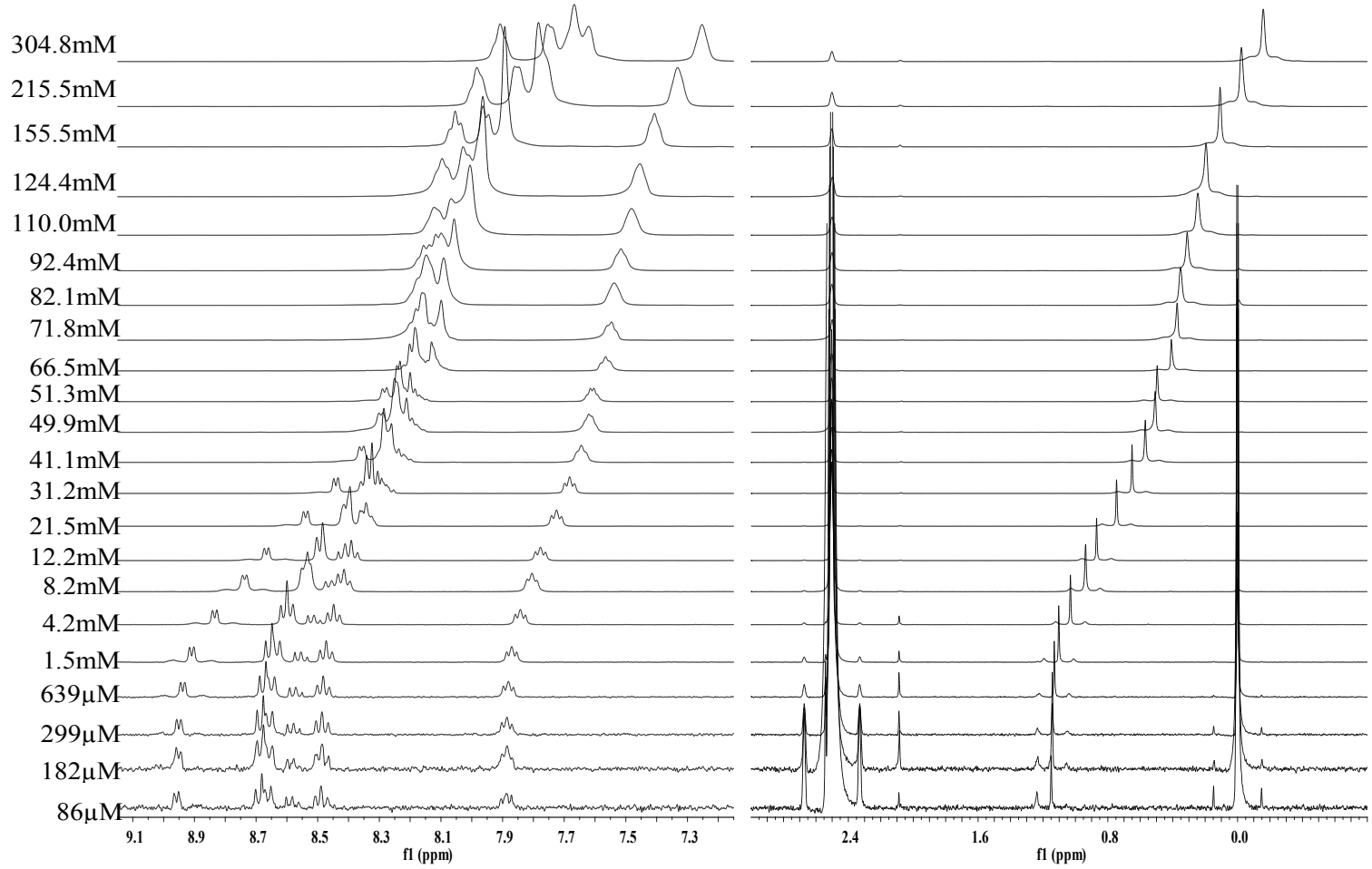

Figure S1: An overlay of ^{1}H NMR spectra of **1** at concentrations ranged from 86 µM – 304 mM in DMSO –d_6 at room temperature. Top spectrum at 304.8 mM is that of the saturated solution (precipitated sample)

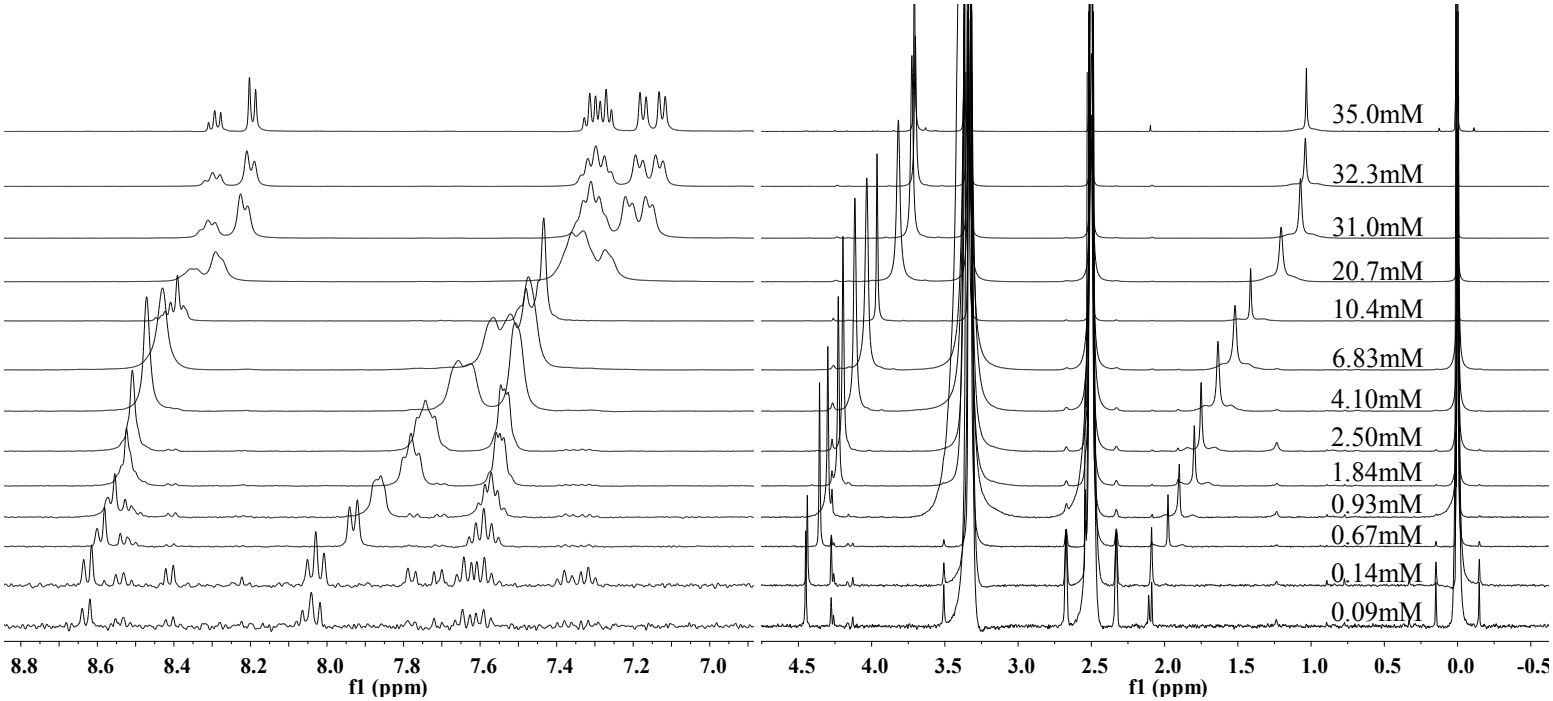

Figure S2: An overlay of ^{1}H NMR spectra of **2** at concentrations ranged from 0.3-35 mM in DMSO-d_6 at room temperature**.**

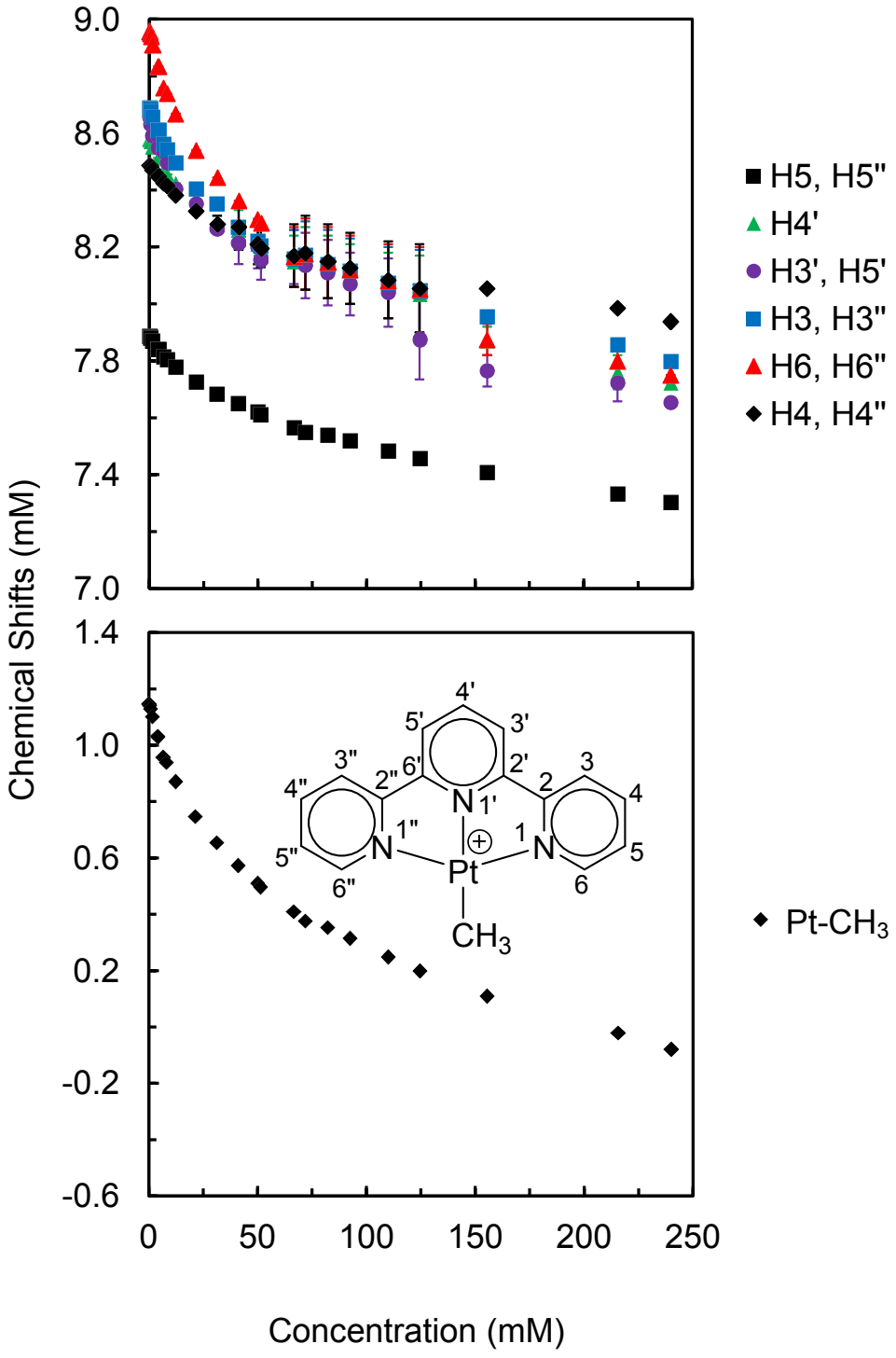

Figure S3. Concentration dependence of ^{1}H chemical shifts of **1** in DMSO-d_6 at room temperature.

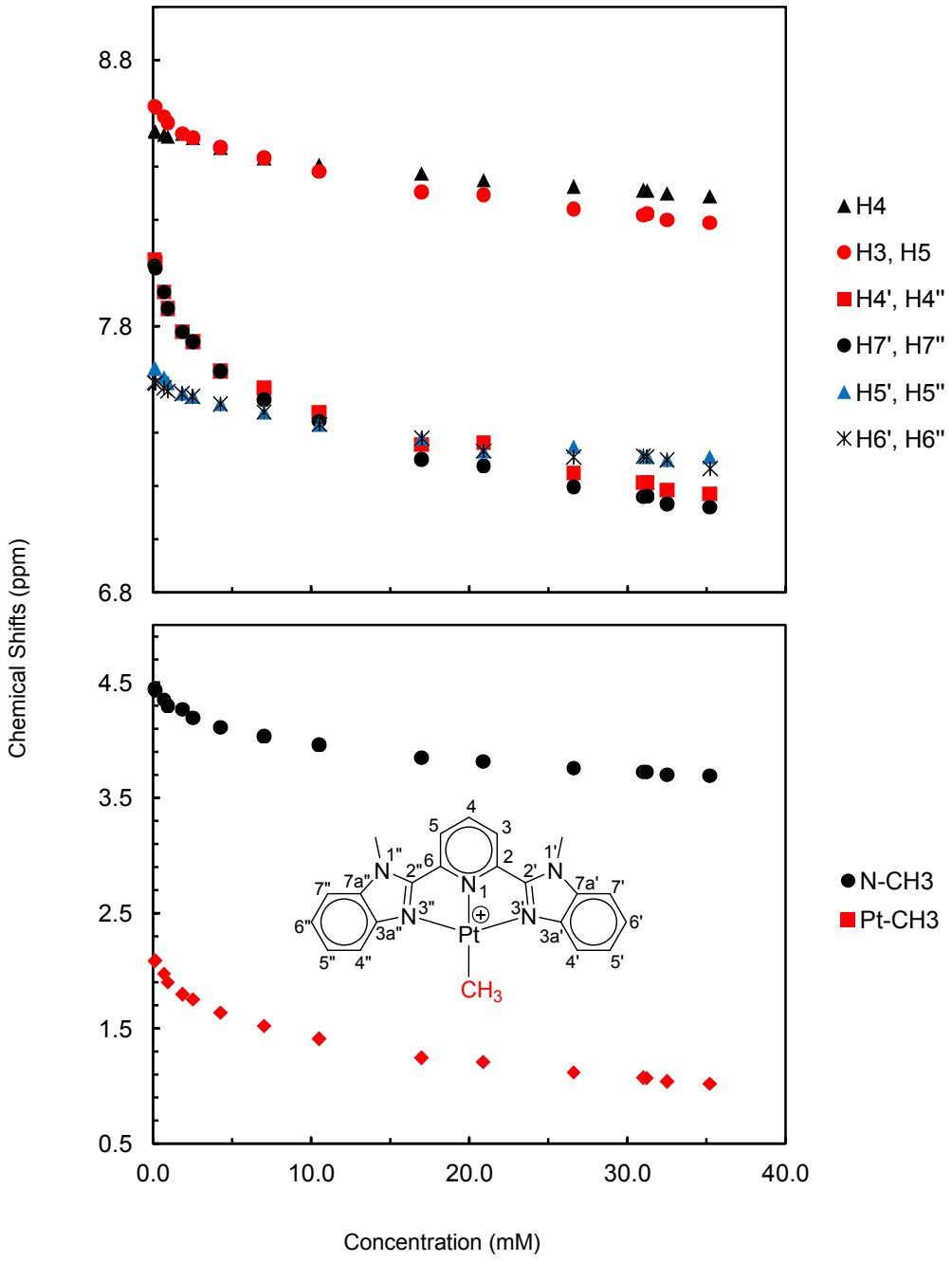

Figure S4: Concentration dependence of ^{1}H chemical shifts of **2** in DMSO-d_6 at room temperature.

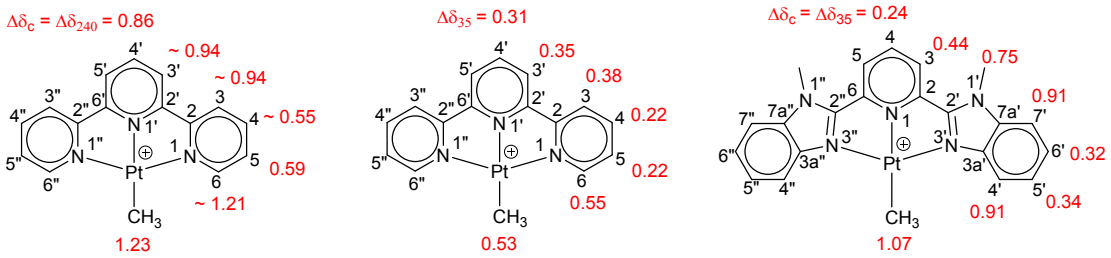

Pt(tpy)CH_3^+, **1** Pt(mbzimpy)CH_3^+ , **2**

Scheme S1. The changes in chemical shifts ($\Delta\delta_c$), shown in red, over the concentration ranges of **86 µM-240 mM** and **86 µM-35 mM** for **1,** and **90 µM-35.2 mM** for **2** in DMSO-d_6**.** Herein, the highest concentration denotes maximum solubility of a compound in DMSO-d_6 solvent and $\Delta\delta_c$ represents the difference in the chemical shift at concentration c (mM) and the lowest investigated concentration (~ 0.09 mM).

^{1}H NMR Data Fitting:

Chemical shift data were fitted according to a model describing the dynamic equilibrium between a monomer (M) and an aggregate (M_n):

$$nM \rightleftharpoons M_n \qquad (1)$$

Where the equilibrium constant, K, is given by:

$$K = \frac{[M_n]}{[M]^n} \qquad (2)$$

It can be shown that the observed chemical shift (δ_{obs}) is given by[10]

$$(\delta_1 - \delta_{obs})C = \frac{(\delta_{obs} - \delta_n)^n}{(\delta_1 - \delta_n)^{n-1}}(nKC^n) \qquad (3)$$

where δ_1 is the chemical shift of the monomer and δ_n is the chemical shift of the aggregate. C is the total concentration of complex (= [M] + n[M_n]).

In the case of n=2, solving for δ_{obs} gives:

$$\delta_{obs} = \frac{-\delta_1(1 \pm \sqrt{1+8CK}) + \delta_2(1+4CK \pm \sqrt{1+8CK})}{4CK} \quad (4)$$

Data were fit to the solution relevant to the current case:

$$\delta_{obs} = \frac{-\delta_1(1 - \sqrt{1+8CK}) + \delta_2(1+4CK - \sqrt{1+8CK})}{4CK} \quad (5)$$

where δ_1, δ_2 and K were fitted parameters.

Models and data of this type suffer from high parameter correlation and parameter effects curvature. For the methyl proton chemical shift data described here, parameter effects curvatures was in the 0.8-1.8 range. A robust approach to fitting these data involved using Chen and Jones' iterative graphical approach[11] implemented in Mathematica 8.0 to obtain initial guesses of values of δ_1, δ_2 and K. These starting parameters were sufficiently close to give good convergence in the ensuing nonlinear least squares regression.

Because of high curvature, confidence intervals calculated using linearization and likelihood methods are slightly (though not greatly) different[12]. Exact 95 % confidence regions were determined by the lack-of-fit method. The regions are bound and not dis-joint. They were determined in an iterative procedure. First, a more-or-less random vector was selected in parameter space, [δ_1, δ_2, K], and the test value was calculated at two positions along this vector. Linear interpolation was used estimate the distance (and therefore new test values of δ_1, δ_2, and K) in this direction that would yield a test value equal to the appropriate F-test statistic. The two nearest points were retained, and the linear interpolation was repeated until the agreement was within 0.3 %. This strategy allowed for reasonably speedy generation of the 95 % confidence boundary in 3-parameter space.

Table S2: Fitting Results for δ (Pt-CH_3) of Pt(tpy)$(CH_3)^+$

	Estimate (linear confidence	Exact Confidence Region	
Parameter	interval)	Lower Bound	Upper Bound
δ_1 (ppm)	1.134±0.014	1.11	1.16
δ_2 (ppm)	-0.96±0.10	-1.20	-0.88
K (M^{-1})	6.15±0.79	4.99	7.58

Table S3: Fitting Results for δ (Pt-CH_3) of Pt(mbzimpy)$(CH_3)^+$

	Estimate (linear confidence	Exact Confidence Region	
Parameter	interval)	Lower Bound	Upper Bound
δ_1 (ppm)	2.09±0.07	2.04	2.14
δ_2 (ppm)	0.40±0.12	0.16	0.57
K (M^{-1})	58.6±15.6	36.9	90.0

Table S4: Fitting Results for δ (N-CH_3) of Pt(mbzimpy)$(CH_3)^+$

	Estimate (linear confidence	Exact Confidence Region	
Parameter	interval)	Lower Bound	Upper Bound
δ_1 (ppm)	4.445±0.025	4.41	4.49
δ_2 (ppm)	3.26±0.09	3.08	3.39
K (M^{-1})	60.6±16.2	37.4	95.1

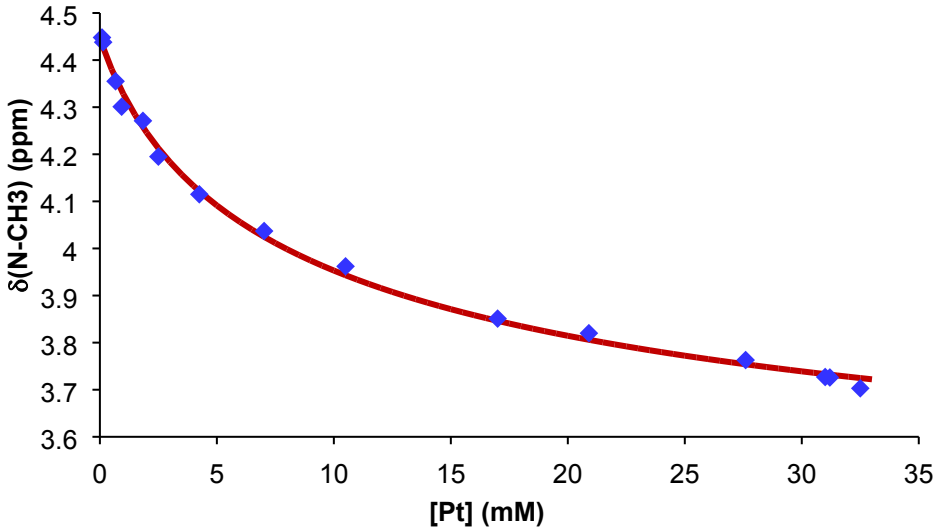

Figure S5: N-methyl proton chemical shift for Pt(mbzimpy)$(CH_3)^+$ vs. concentration. Red line shows best fit to a monomer-dimer dynamic equilibrium model (R^2=0.99998).

Visible absorption data fitting:

The absorption data of **1** and **2** at 560-nm were fitted to a model describing the dynamic equilibrium between a monomer (M) and a dimer (M_2).

$$2M \rightleftharpoons M_2 \quad (6)$$

As noted by *Bailey et al.,*[13] dimerization is expected to result in a linear dependence of $[Pt]/\sqrt{A}$ on $\sqrt{A}$ as illustrated by:

$$\frac{[Pt]}{\sqrt{A}} = \frac{1}{\sqrt{\epsilon K}} + \frac{2}{\epsilon}\sqrt{A} \quad (7)$$

Where, [Pt] = total concentration of the complex, A= absorbance, ε = molar absorptivity, and K = dimerization constant.

Table S5: Fitting results for 560-nm absorptions of **1** and **2.**

	1	**2**
K (M^{-1})	17 ±2	72 ±4
ε (M^{-1} cm^{-1})	354 ±1	476 ±1

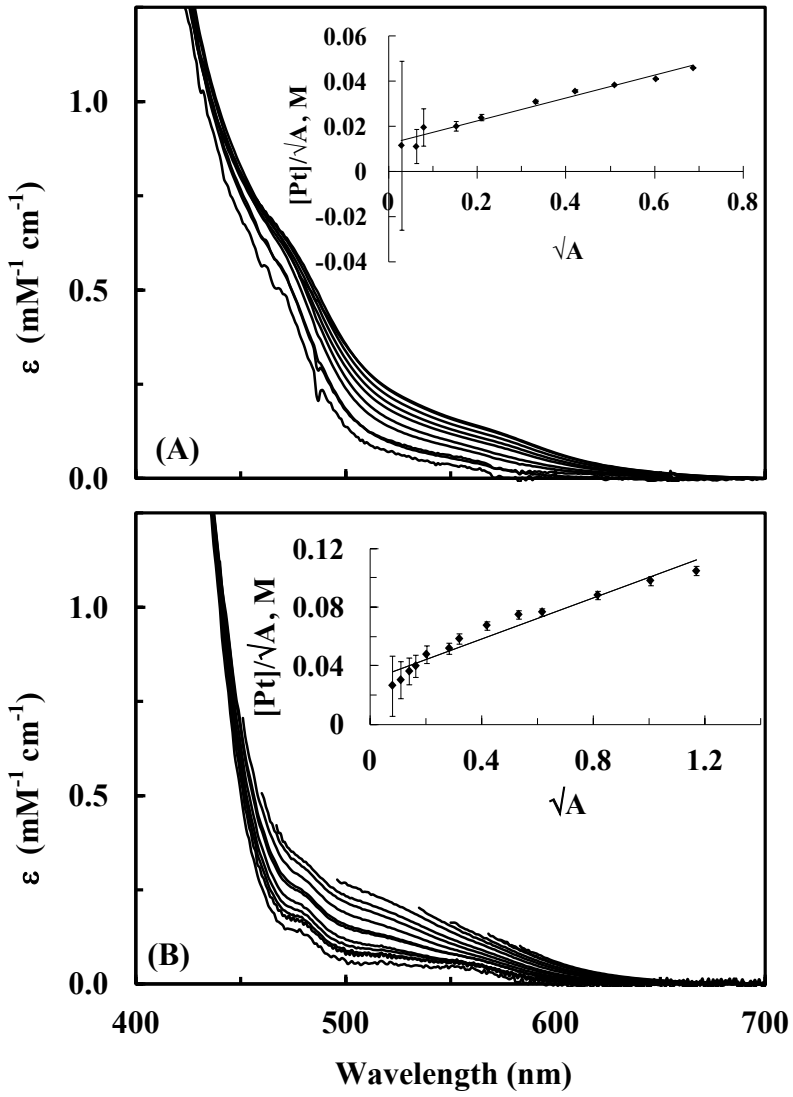

Figure S6: Electronic absorption spectra of (A) **2** at concentration ranged from 0.3-32 mM in DMSO solution (Inset: Dimerization plot of **2** for the concentration range 0.3-32 mM using the 560-nm band. Error bars represent ± 2σ. Line shows linear weighted least squares fit according to eq. $[Pt]/\sqrt{A} = 1/\sqrt{\epsilon K} + 2/\epsilon\sqrt{A}$: slope = 41.99 x 10^{-3} ± 0.74 cm^{-1}; intercept = 17.10 x 10^{-3} ± 0.44), and (B) **1** at concentration ranged from 3-200 mM. Inset: Dimerization plot of **1** for the concentration range 3-122 mM using 560-nm band. Slope = 56.56 x 10^{-3} ± 3.41; intercept = 41.14 x 10^{-3} ± 2.29

Despite the fact that 560-nm absorption data fit reasonably well in one dimer model illustrated by equation 6, the molar absorptivity (**ε**) of this 560-nm band, if assumed to be originated from ^{1}MMLCT state, is low in comparison to the **ε** of 2000 - 4000 $M^{-1}cm^{-1}$ reported for the corresponding band of authentic Pt..Pt dimers.[13-16] By this reason, it is likely that additional dimer(s) that is lacking Pt..Pt interaction (or π..π dimer) was formed in solution. By taking a similar approach used by *Bailey et al.*[13], a two dimer model as illustrated by equations 8 and 9 was applied to the 560-nm fits (Fig S6). From this data treatment, dimerization constants (K_{MM} and $K_{\pi\pi}$) were estimated under an assumption that ε_{MM} for Pt...Pt dimer is about 2000 $M^{-1}cm^{-1}$.

$$2Pt \rightleftharpoons (Pt_2)_{MM} \quad (8)$$

$$2Pt \rightleftharpoons (Pt_2)_{\pi\pi} \quad (9)$$

$$\frac{[Pt]}{\sqrt{A}} = \frac{1}{\sqrt{\epsilon_{MM}K_{MM}}} + \left(\frac{2}{\epsilon_{MM}} + \frac{2K_{\pi\pi}}{\epsilon_{MM}K_{MM}}\right)(\sqrt{A}) \quad (10)$$

Where,

ε_{MM} : molar absorptivity of metal..metal dimer,

K_{MM} : dimerization constant for metal..metal dimer,

$K_{\pi\pi}$: dimerization constant for π..π dimer.

Table S6: Fitting results for 560-nm absorptions of **1** and **2** by applying a two dimer model**.**

	1[a]	**2**[a]
K_{MM} (M^{-1})	3 ±0	17 ±3
$K_{\pi\pi}$ (M^{-1})	14 ±2	55 ±10

[a] By assuming that ε_{MM} at λ, 560-nm is 2000 M^{-1} cm^{-1}

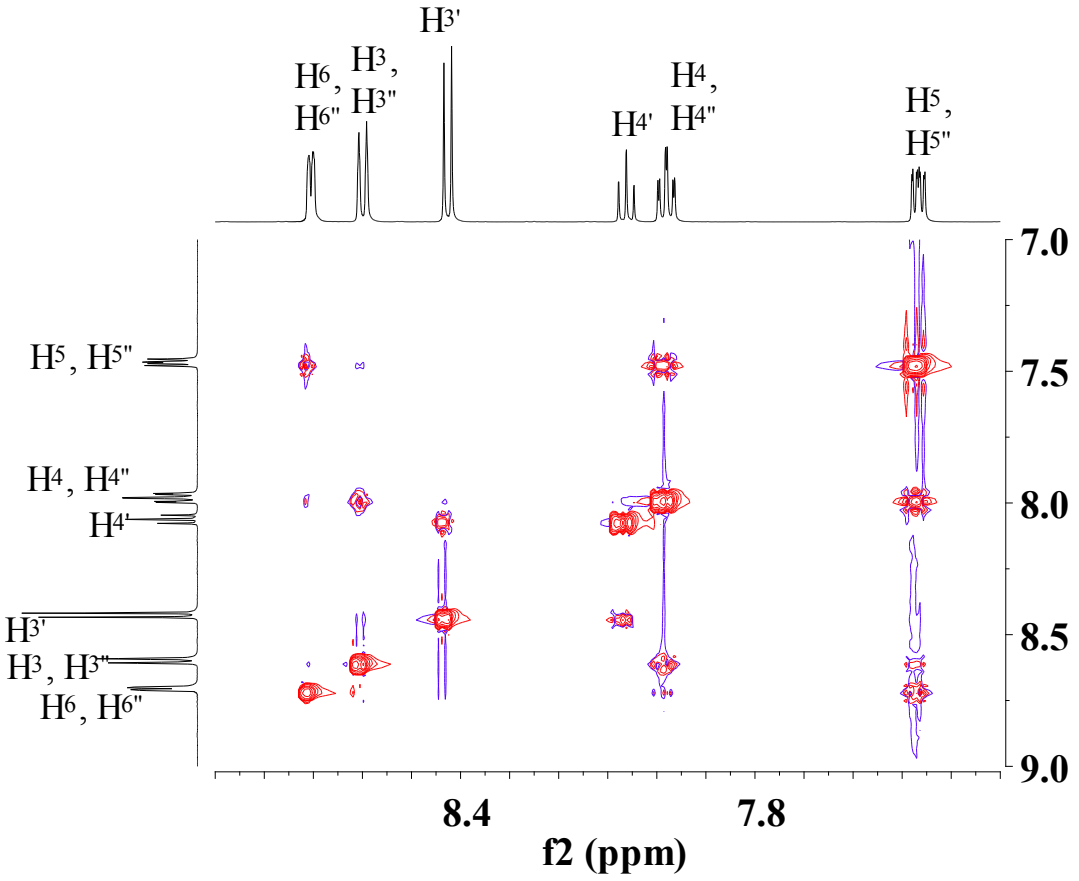

Figure S7: 2D ^{1}H-^{1}H NOESY spectrum of terpyridine (311 mM solution) in DMSO-d_6 at RT.

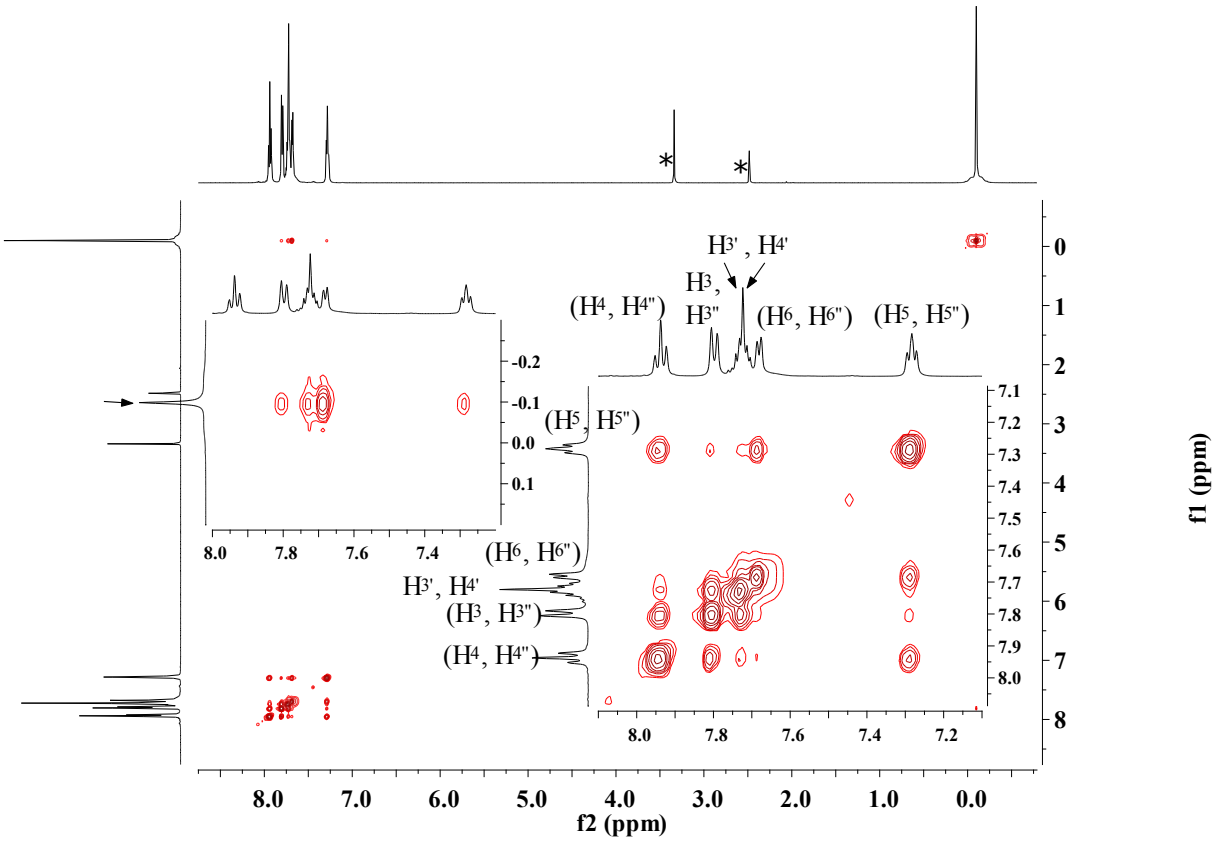

Figure S8: 2D ^{1}H-^{1}H NOESY spectrum of **1** (240 mM) in DMSO-d_6 at RT. Insets: Partial 2D NOESY spectra of **1**.

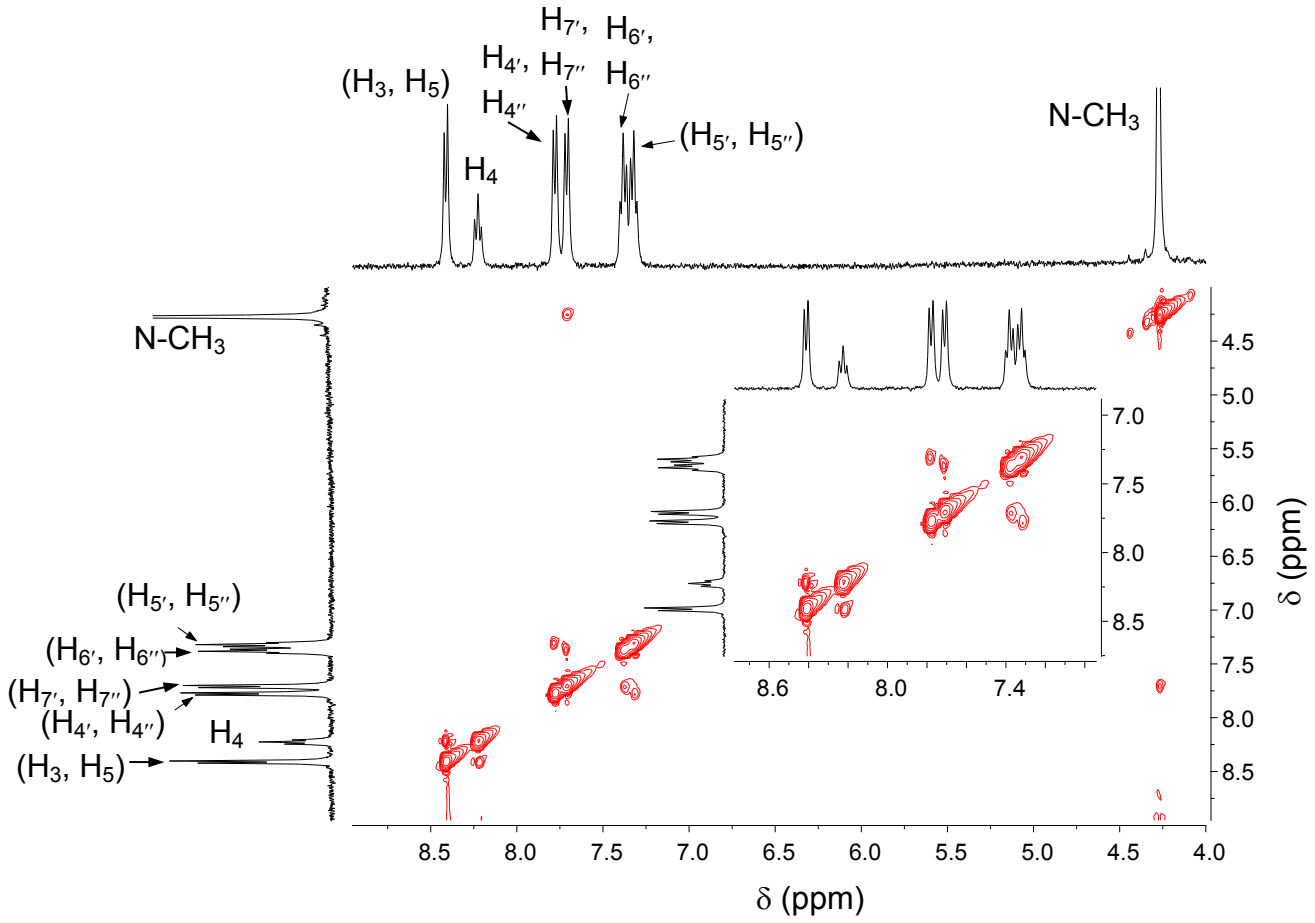

Figure S9: 2D NOESY spectrum of mbzimpy in DMSO-d_6 at RT.

REFERENCES

1. A. W. Addison, S. Burman, C. G. Wahlgren, O. A. Rajan, T. M. Rowe and E. Sinn, *J. Chem. Soc., Dalton Trans.*, 1987, 2621-2630.
2. J. X. McDermott, J. F. White and G. M. Whitesides, *J. Am. Chem. Soc.*, 1976, **98**, 6521-6528.
3. C. Eaborn, K. J. Odell and A. Pidcock, *J. Chem. Soc., Dalton Trans.*, 1978, 357-368.
4. G. S. Hill, M. J. Irwin, C. J. Levy, L. M. Rendina and R. J. Puddephatt, *Inorg. Synth.*, 1998, **32**, 149-153.
5. R. J. Cross and M. F. Davidson, *J. Chem. Soc., Dalton Trans.*, 1986, 1987-1992.
6. H. E. Gottlieb, V. Kotlyar and A. Nudelman, *J. Org. Chem.*, 1997, **62**, 7512-7515.

7. V. M. Shingade, L. J. Grove and W. B. Connick, *Dalton Trans.*, 2020, DOI: 10.1039/d0dt01496f.
8. G. Arena, G. Calogero, S. Campagna, L. M. Scolaro, V. Ricevuto and R. Romeo, *Inorg. Chem.*, 1998, **37**, 2763-2769.
9. G. Arena, L. M. Scolaro, R. F. Pasternack and R. Romeo, *Inorg. Chem.*, 1995, **34**, 2994-3002.
10. G. Jones and V. I. Vullev, *J. Phys. Chem. A*, 2001, **105**, 6402-6406.
11. J. S. Chen and R. B. Shirts, *J. Phys. Chem.*, 1985, **89**, 1643-1646.
12. David A. Ratkowsky "Handbook of Nonlinear Regression Models," Marcel Dekker Inc. New York, 1990
13. J. A. Bailey, M. G. Hill, R. E. Marsh, V. M. Miskowski, W. P. Schaefer and H. B. Gray, *Inorg. Chem.*, 1995, **34**, 4591-4599.
14. J. A. Bailey, V. M. Miskowski and H. B. Gray, *Inorg. Chem.*, 1993, **32**, 369-370.
15. E. M. A. Ratilla, B. K. Scott, M. S. Moxness and N. M. Kostic, *Inorg. Chem.*, 1990, **29**, 918-926.
16. K. M.-C. Wong, N. Zhu and V. W.-W. Yam, *Chem. Commun.*, 2006, DOI: 10.1039/b606352g, 3441-3443.